Two-Electron Dissociative Ionization of H_2 and D_2 in Infrared Laser Fields

P. Dietrich,[1] M. Yu. Ivanov,[2] F. A. Ilkov,[3] and P. B. Corkum[2]
[1]*Institut für Experimentalphysik, Freie Universität Berlin, 14195 Berlin, Germany*
[2]*Steacie Institute for Molecular Sciences M-23A, National Research Council of Canada, Ottawa, Ontario, K1A 0R6, Canada*
[3]*Centre d'Optique, Photonique et Laser, Université de Laval, Québec, Québec, G1K 7P4, Canada*
(Received 12 February 1996)

We present a quantitative physical model of above-threshold dissociation of homonuclear molecular ions in intense midinfrared laser fields. This allows us to describe self-consistently all three processes that occur during dissociative ionization of H_2 and D_2 (ionization of the neutral molecule, dissociation of the molecular ion, and its secondary ionization) using a semiclassical approach. The kinetic energy spectrum of the dissociating fragments is obtained and analyzed. [S0031-9007(96)01645-6]

PACS numbers: 33.80.Rv, 82.50.Fv

We develop a quantitative physical model of the dissociation of homonuclear molecular ions (e.g., H_2^+) in intense midinfrared laser fields and show how laser-induced electron motion influences the nuclear dynamics. For homonuclear ions which do not have a permanent dipole moment, above-threshold dissociation is not analogous to well-studied above-threshold ionization of atoms, but a qualitatively different physical process. Energy accumulation by the dissociating nuclei occurs at small internuclear distances through the induced dipole moment. It is halted at larger distances, when the electron tunneling time between the dissociating nuclei becomes too long for the electron to respond to the oscillating electric field. Giving a clear understanding of the underlying physics of above-threshold dissociation is the main aim of this paper.

Development of a complete self-consistent model of two-electron dissociative ionization of H_2 and D_2, including both the first ($H_2 \rightarrow H_2^+$) and the second ($H_2^+ \rightarrow H_2^{2+}$) ionization steps, is the second aim of this paper. Signatures of different aspects of the dissociative ionization are identified in the kinetic energy spectrum of the molecular fragments.

A self-consistent model is important because intense-field experiments start with neutral molecules and measure the kinetic energy spectrum of the charged fragments. Therefore, in the case of H_2 or D_2, one has to include the ionization of both electrons and the nuclear dynamics. Such *ab initio* calculations far exceed the capacity of modern computers. Excellent recent work [1] on intense-field dissociation of H_2^+ and HD^+ at 10 μm does not include either of the two ionization steps. The first *ab initio* study to include dissociation of H_2^+, together with its subsequent ionization (one ionization step) [2], is limited to UV and visible frequencies. The Floquet picture, successfully used for moderate laser intensities and wavelengths $\lambda \leq 1\ \mu$m [3], can, in principle, be generalized to include both ionization steps. However, it becomes impractical in intense ($I \sim 10^{14}\ \mathrm{W\,cm^{-2}}$) midinfrared (10 μm) fields.

The long-wavelength limit offers a major simplification in the treatment of dissociative ionization. It allows us to use the quasistatic model, so successful for calculating intense-field atomic above-threshold ionization [4] and molecular dissociation thresholds [5,6] at 10 μm. The physics of above-threshold dissociation in the long-wavelength limit is as follows. At small internuclear distances the electron instantaneously responds to the oscillations of the external field $\mathcal{E}(t) = \mathcal{E}_0 \cos \omega t$, tending to flow towards one nucleus or the other. Averaged over the laser cycle, that results in a net force pulling the nuclei apart. For a dissociating molecular ion, this is the stage during which the nuclei gain energy from the laser field. As the internuclear separation R increases, the electron can no longer adiabatically respond to the electric field. Physically, the internal potential barrier between the two nuclei increases, and tunneling of the electron through the barrier during the laser cycle becomes exponentially small. Tunneling is even more suppressed by the intense laser field [7]. As a result, the electron localizes near one of the nuclei, leaving the other nucleus oscillating in the laser field. Averaged over the laser cycle, the net force pulling the nuclei apart decreases exponentially with R. This completes above-threshold dissociation: No further energy is absorbed from the laser field.

The same physical processes are also important for the alignment dynamics. As long as the electron adiabatically responds to the oscillations of $\mathcal{E}_0 \cos \omega t$, the induced dipole moment $\mu(\mathcal{E})$ follows the electric field and the $\mu \times \mathcal{E}$ force tends to align the ion during the whole laser cycle. Electron localization freezes $\mu(\mathcal{E})$, and the $\mu \times \mathcal{E}$ force, averaged over one laser cycle, becomes equal to zero.

We now present a mathematical description of dissociative ionization. In the first step, the neutral molecule is ionized. We use standard tunnel ionization models [8] shown to accurately describe ionization of small neutral molecules [5]. Ionization is a vertical transition and is calculated at each phase of the laser field.

To describe the second step of dissociative ionization, we use classical mechanics for the motion of the nuclei while treating the electron dynamics quantum mechanically. An ensemble of trajectories is launched on the lower quasistatic ionic surface given by Eq. (1) (see below). The initial conditions are thus given by the initial internuclear distances and velocities on the neutral vibrational ground state, weighted by the laser phase dependent ionization rate and the ground state vibrational wave function of the neutral molecule. We also take into account that the ionization rate is R dependent owing to the R-dependent energy of vertical transition to the lowest quasistatic ionic surface.

We now formulate the quantitative model of above-threshold dissociation. For H_2^+ (D_2^+) only the two lowest-lying potential surfaces, σ_g and σ_u, have to be considered [1,2]. Strong charge-resonance coupling with transition matrix element $\mu(R) \approx eR/2$ [9] mixes these states and is responsible for the dissociation of the molecular ion in a 10 μm laser field [5,6,10]. The quasistatic potential surfaces are given by

$$E_{1,2}(R,t) = \frac{E_1^0(R) + E_2^0(R)}{2} \mp \sqrt{\frac{\Delta E_{12}^2(R)}{4} + V^2(R,t)}\,. \tag{1}$$

$E_{1,2}^0(R)$ are the field-free ground (gerade σ_g) and excited (ungerade σ_u) potential surfaces, $V(R,t) = -\mu(R)\mathcal{E}(t)$ is the coupling between them, $\mathcal{E}(t) = \mathcal{E}_0(t)\cos\omega t$, and $\Delta E_{12}(R) = E_2^0(R) - E_1^0(R)$. In a strong field the bond is weakened [11] [see Fig. 1(a)]. This is the long-wavelength limit of the bond softening picture [12]. As long as the dissociating ion stays on the lower quasistatic surface, it gains the energy from the field, see Fig. 1(a). For a given surface, the force on the molecular ion is given by the derivative $-\partial E_i(R,t)/\partial R$ and is purely deterministic.

The probability for nonadiabatic transitions between the quasistatic potential surfaces is critical. In intense 10 μm light, these transitions occur at quite large R and near zeros of the instantaneous field, $\cos\omega t \approx 0$, see below. The transition probability $P_{\mathrm{trans}}(R)$ is shown in Fig. 1(b). When $P_{\mathrm{trans}}(R)$ reaches unity, electron localization is complete and energy gain ceases. Instantaneous transitions between the quasistatic surfaces introduce a stochastic aspect to the dynamics in the intermediate region [see Fig. 1(b)]. At large R, where $P(R) = 1$, the force on the molecule is again deterministic and describes wiggling of the ion in the laser field.

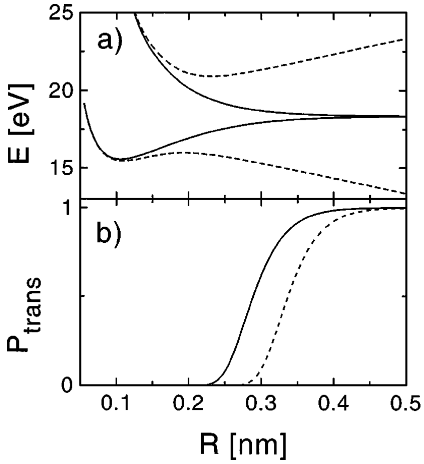

FIG. 1. (a) Quasistatic potential curves for H_2^+ (D_2^+) without field (solid curve) and with an external dc field of 20 V nm^{-1} (dashed). (b) Transition probability $P_{\mathrm{trans}}(R)$ between the quasistatic states during one laser half-cycle. $\lambda = 10$ μm, $I = 1.3 \times 10^{13}$ W cm^{-2} (dashed) and $I = 3.3 \times 10^{14}$ W cm^{-2} (solid).

To derive $P_{\mathrm{trans}}(R)$ we note that, at small internuclear distances, $\hbar\omega \ll \Delta E_{12}(R)$ and $V_0(R)\hbar\omega \ll \Delta E_{12}^2(R)$, where $V_0(R) = \mu(R)\mathcal{E}_0(t)$. Under these conditions, transitions between the quasistatic states $E_{1,2}(R,t)$ are negligible [13]. For H_2^+ and intensities of some 10^{13} W cm^{-2}, this is the case for $R < 0.3$ nm [see Fig. 1(b)]. As R increases, we reach a region where $\Delta E_{12}^2(R) \sim V_0(R)\hbar\omega$ and nonadiabatic transitions become important. For intense 10 μm light in this region of internuclear distances, $V_0(R) \gg \Delta E_{12}(R)$. There it is convenient to rewrite the Schrödinger equation in the basis $|l\rangle = (|1\rangle + |2\rangle)/\sqrt{2}$ and $|r\rangle = (|1\rangle - |2\rangle)/\sqrt{2}$. These states correspond to the electron staying either with the left or the right nucleus. Equations for the probability amplitudes in the states $|l\rangle$ and $|r\rangle$ immediately show that the transitions between $|l\rangle$ and $|r\rangle$ occur when $|2V(R,t)| \leq \Delta E_{12}(R)$. Combined with the condition $V_0(R) \gg \Delta E_{12}(R)$, it means $|\cos\omega t| \ll 1$, justifying hopping at zero field.

Expanding $V(R,t)$ near $\cos\omega t = 0$ for the probability $P_{\mathrm{lr}}(R)$ of transition between $|l\rangle$ and $|r\rangle$ during one passage through $\cos\omega t = 0$ we obtain the Landau-Zener-type formula: $P_{\mathrm{lr}}(R) = 1 - \exp[-\gamma(R)]$, where

$$\gamma(R) = \pi\Delta E_{12}^2(R)/4\hbar\omega V_0(R)\,. \tag{2}$$

Transforming back to the quasistatic basis, P_{lr} is the probability of staying on the same quasistatic surface. Consequently, the probability of nonadiabatic transition between the quasistatic states *during one laser half cycle* is $P_{\mathrm{trans}}(R) = 1 - P_{\mathrm{lr}}(R) = \exp[-\gamma(R)]$.

In our semiclassical approach we neglect interference between transitions that can occur during successive laser half-cycles. In a two-level system without nuclear motion such interference is essential. However, in the 16 fs (laser half-cycle) between the nonadiabatic transitions, the nuclear trajectories on the upper and lower quasistatic surfaces diverge, so that they do not overlap at the time of the next nonadiabatic transition. Furthermore, for typical kinetic energies of the dissociating fragments $K \sim 1$ eV, the R-dependent *nuclear phase* accumulated during the laser half-cycle is $\delta\phi(R,t) \sim 20\pi$. Hence, although interference is present in principle, it is highly complex and should average out.

The third and final step needed to completely solve the problem of dissociative ionization of H_2 is the ionization of the molecular ion. It has been studied recently [14–16], and we summarize the physical principles. Ionization is most efficient from the upper quasistatic surface, whose population depends critically on the electron localization. If the molecular ion is on the upper surface, the electron is in the upper well of the quasistatic potential $U(x, R, \mathcal{E}) = -Qe/|x - R/2| - Qe/|x + R/2| - e\mathcal{E}x$, where the nuclear charge $Q = e$ in our case. Then, for sufficiently large R, the electron tunneling to the continuum occurs directly through the *inner* barrier between the wells of $U(x, R, \mathcal{E})$ [14–16] in a *combined* electric field of the laser and the adjacent atomic ion [14]. To implement this effect in our quantitative analysis, we obtain an analytical formula by mapping [14] ionization from the double-well potential $U(x, R, \mathcal{E})$ to a well-known atomic tunnel ionization problem [8]. To first approximation, this results in introducing an effective ionization potential $I_{p,\mathrm{eff}}(R, \mathcal{E})$ and an effective electric field $\mathcal{E}_{\mathrm{eff}}(R)$:

$$\begin{aligned} I_{p,\mathrm{eff}}(R, \mathcal{E}) &\approx \frac{I_{p,1}(R) + I_{p,2}(R)}{2} \\ &\quad - \frac{Qe}{|R - x_0|} + \frac{Qex_0}{|R - x_0|^2}, \\ \mathcal{E}_{\mathrm{eff}}(R) &= \mathcal{E} + \frac{Q}{|R - x_0|^2}, \end{aligned} \qquad (3)$$

where $x_0 = x_0(R, \mathcal{E})$ is the top of the barrier between the wells and $I_{p,i}(R)$ are the field-free ionization potentials from gerade and ungerade states. In our calculations, for each laser phase we use standard atomic dc tunnel ionization rates [8] with $I_{p,\mathrm{eff}}$ and $\mathcal{E}_{\mathrm{eff}}$ given by Eq. (3), and also take into account tunneling through the outer barrier of $U(x, R, \mathcal{E})$, calculated according to [5].

We now concentrate on the results of our calculations. For clarity, we assume the molecule to be aligned along the laser electric field. Both theory [1] and experiment [10,17] show this to be a good approximation: Only aligned fragments are typically observed.

All calculations were performed using a Gaussian pulse of 2.5 ps full-width at half maximum. We launched 2000 trajectories for intensities above 2×10^{14} W cm^{-2} and increased this number with decreasing intensity up to 6×10^5 at the lowest intensity used. In the numerical code, transitions between the quasistatic states occur at $\cos \omega t = 0$ if $P_{\mathrm{trans}}(R) = \exp[-\gamma(R)]$ is larger than a random number. If secondary ionization is neglected, the trajectories are calculated up to $R = 1$ nm from where the molecular potential is negligible. If secondary ionization is included, the calculations are extended to 10 nm to obtain accurate kinetic energies. The final energies are calculated taking the laser field turnoff into account.

Figure 2 shows the kinetic energy spectra of the fragments after dissociative ionization of H_2 and D_2. In Fig. 2(a), secondary ionization is not included in the calculations whereas Figs. 2(b) and 2(c) illustrate its importance for dissociation in 10 μm light. Without secondary ionization the mean energy is approximately given by the energy difference on the lower quasistatic surface between the peak of the barrier [Fig. 1(a)] and the region where electron localization occurs [Fig. 1(b)]. This energy difference increases with increasing the laser field. Our trajectory calculations support this interpretation as shown in Fig. 3, which depicts the intensity dependence of the mean fragment energy for both H_2 and D_2.

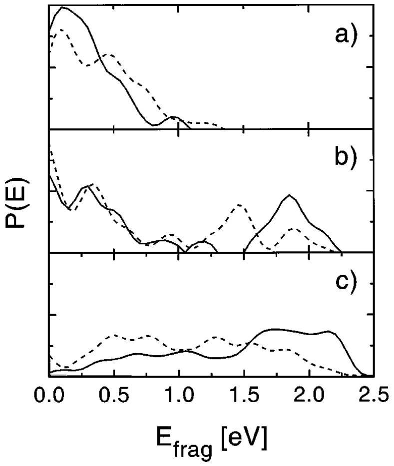

FIG. 2. Kinetic energy distribution of fragments after dissociative ionization of H_2 (dashed) and D_2 (solid) with 10 μm, 2.5 ps laser pulses, smoothed with 0.05 eV resolution. (a)—secondary ionization not included, (b),(c)—secondary ionization included. $I = 8 \times 10^{13}$ W cm^{-2} (a), $I = 6 \times 10^{13}$ W cm^{-2} (b), $I = 1 \times 10^{14}$ W cm^{-2} (c).

Figures 2(b) and 2(c) show the modification of the kinetic energy distribution due to secondary ionization which peaks strongly near $R \sim 0.4$–0.5 nm, where tunneling through the inner barrier of $U(x, R, \mathcal{E})$ directly to the continuum is most efficient. Passing through this "critical" region of internuclear distances, molecular ions

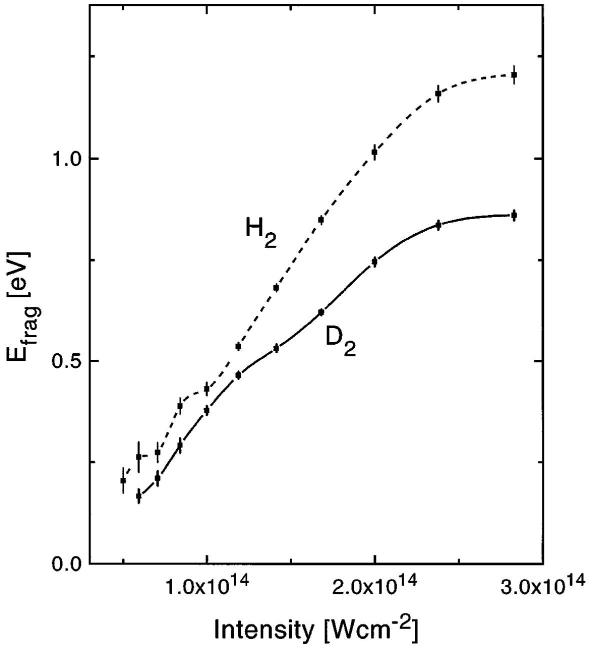

FIG. 3. Intensity dependence of the mean kinetic energy of fragments after dissociative ionization of H_2 and D_2 with 10 μm, 2.5 ps laser pulses. As in Fig. 2(a), secondary ionization is not included to illustrate the physical mechanism of the above-threshold dissociation.

are further ionized, yielding a well defined high-energy peak [Fig. 2(b)]. The modification of the spectrum is much stronger for higher intensities due to the highly nonlinear nature of secondary ionization. The effect is also stronger for D_2, since the heavier deuteron needs longer time to move through the region of efficient ionization.

Our results can be compared with the first experiments on 10 μm dissociative ionization of H_2 and D_2 [10], where kinetic energies of fragments were studied. Although the experimental setup did not allow for detailed quantitative measurements of kinetic energy distributions, a qualitative comparison of the main spectrum features is possible. The characteristic fragment energies measured in [10] (0.7 eV for H^+, 0.6 eV for D^+) are similar to our data, although the much longer experimental pulse duration (2.5 ns vs 2.5 ps) prevents an exact comparison. A striking experimental observation, also predicted by our calculations, is the appearance of a high-energy peak at 2.2 eV in the D^+ energy spectrum, while such a peak is nearly absent for H^+. Our calculations show that the probability for secondary ionization is lower for H_2^+ than for D_2^+ and that the energy distribution of H^+ is flatter than that of D^+ and has a less pronounced high-energy peak [see Figs. 2(b) and 2(c)]. At higher intensities the fragment spectrum of H_2 becomes even flatter, while D_2 exhibits a distinct high-energy peak with growing relative height, Fig. 2(c).

In conclusion, we have developed a quantitative physical model of above-threshold dissociation and a self-consistent model of two-electron dissociative ionization of H_2 (D_2). The fragments gain energy until transitions between the quasistatic states become efficient. Transitions occur beyond a critical internuclear separation, $R > R_{\mathrm{cr}}$. The magnitude of the field and/or its direction at the moment when the nuclei pass R_{cr} can be controlled by varying the wavelength or coherently mixing two laser frequencies. This will control the kinetic energy spectrum of the fragments, probability of secondary ionization, and the branching ratio in dissociation of molecular ions.

We thank S. L. Chin, T. Walsh, D. Wardlaw, M. Thachuk, A. Bandrauk, T. Zuo, and D. D. Normand for fruitful discussions. M. I. acknowledges financial support of NSERC special collaborative research grant. F. I. acknowledges financial support of NSERC and NATO linkage grant.

[1] E. Charron, A. Giusti-Suzor, and F. H. Mies, Phys. Rev. Lett. **75**, 2815 (1995); see also *ibid.* **71**, 692 (1993).
[2] S. Chelkowski *et al.,* Phys. Rev. A **52**, 2977 (1995).
[3] See, e.g., *Molecules in Laser Fields*, edited by A. Bandrauk (Marcel Dekker, New York, 1994).
[4] P. B. Corkum, N. H. Burnett, and F. Brunel, Phys. Rev. Lett. **62**, 1259 (1989); S. Augst *et al.,* Phys. Rev. Lett. **63**, 2212 (1989).
[5] P. Dietrich and P. B. Corkum, J. Chem. Phys. **97**, 3187 (1992).
[6] M. Thachuk and D. Wardlaw, J. Chem. Phys. **102**, 7462 (1995).
[7] See, e.g., F. Grossmann *et al.,* Phys. Rev. Lett. **67**, 516 (1991); R. Bavli and H. Metiu, Phys. Rev. Lett. **69**, 1986 (1992); M. Holthaus, Phys. Rev. Lett. **69**, 1596 (1992).
[8] A. M. Perelomov, V. S. Popov, and M. V. Terent'ev, Sov. Phys. JETP **23**, 924 (1966); M. V. Ammosov, N. B. Delone, and V. P. Krainov, *ibid.* **64**, 1191 (1986).
[9] R. S. Mulliken, J. Chem. Phys. **7**, 20 (1939).
[10] F. A. Ilkov *et al.,* Phys. Rev. A **51**, R2695 (1995); F. A. Ilkov *et al.,* Chem. Phys. Lett. **247**, 1 (1995).
[11] G. R. Hanson, J. Chem. Phys. **62**, 1161 (1972).
[12] P. H. Bucksbaum *et al.,* Phys. Rev. Lett. **64**, 1883 (1990); A. Zavriyev *et al.,* Phys. Rev. A **42**, 5500 (1990).
[13] See, e.g., V. P. Krainov and V. P. Yakovlev, Sov. Phys. JETP **51**, 1104 (1980); I. Sh. Averbukh and N. F. Perelman, *ibid.* **61**, 665 (1985).
[14] T. Seideman, M. Yu. Ivanov, and P. B. Corkum, Phys. Rev. Lett. **75**, 2819 (1995); M. Yu. Ivanov *et al.,* Phys. Rev. A **54**, 1541 (1996).
[15] T. Zuo and A. Bandrauk, Phys. Rev. A **52**, R2511 (1995).
[16] K. Codling, L. J. Frasinski, and P. A. Hatherly, J. Phys. B **22**, L321 (1989); J. H. Posthumus *et al.,* J. Phys. B **28**, L349 (1995).
[17] L. J. Frasinski *et al.,* Phys. Rev. Lett. **58**, 2424 (1987); D. Strickland *et al.,* Phys. Rev. Lett. **68**, 2755 (1992); M. Schmidt, D. Normand, and C. Cornaggia, Phys. Rev. A **50**, 5037 (1994).